The Science of the Total Environment, 75 (1988) 285–300
Elsevier Science Publishers B.V., Amsterdam — Printed in The Netherlands

SURFACE pH, SATELLITE IMAGERY AND VERTICAL MODELS IN THE TROPICAL OCEAN

ALBERTO ZIRINO, PAUL C. FIEDLER[1] and ROBIN S. KEIR[2]

Naval Ocean Systems Center, San Diego, San Diego, CA 92152 (U.S.A.)
[1] National Marine Fisheries Center, La Jolla, CA 92093 (U.S.A.)
[2] Scripps Institution of Oceanography, La Jolla CA 92093 (U.S.A.)

ABSTRACT

The relationships between surface pH, ocean color and surface temperature are discussed conceptually. As an example, log pigment and sea-surface temperature (SST) obtained from color and IR satellite imagery collected over the Gulf of California (Mexico) in November 1981 are compared with in situ pH and temperature measurements made 3 weeks later. Plots of log pigment vs. SST and pH vs. in situ temperature show a characteristic break in slope, suggesting that the area studied may be divided into a high productivity northern section and a southern section of correspondingly lower productivity. A multidisciplinary (physical–chemical–biological), one-dimensional (vertical) model is used to produce characteristic shapes of log pigment vs. SST and pH vs. in situ temperature plots.

INTRODUCTION

The development of space-based systems for ocean exploration has presented oceanographers with the opportunity to monitor the ocean's surface synoptically over distances from tens to thousands of kilometers. The two properties most commonly observed with satellites are sea surface temperature (SST) and upwelled color, computed as pigment, which in oceanic waters is a measure of the abundance of phytoplankton in the upper 10–40 m (Gordon et al., 1980, 1983). In tropical waters, the concentration of phytoplankton is related to the quantity of nutrient-rich subsurface water which penetrates the photic zone and the duration of its exposure to solar radiation. Because these latter parameters are controlled by upwelling and turbulent mixing, complex relationships exist between hydrography and satellite-measured temperature and color.

Knowledge of surface–subsurface relationships extends the usefulness of the imagery and provides the theoretical framework for ocean monitoring from space. Such monitoring is much more economical than surveys by ship. At present, data bases for developing algorithms which link subsurface structure to imagery are provided by oceanographic expeditions in which surface (mixed layer) properties are continuously sampled by underway ships as the imagery is collected (Zirino, 1985). Thus, the distances that can be surveyed by the ships

0048-9697/88/$03.50

in a few days approach these covered in the imagery. Ship's surface observations are also augmented with XBT drops and by frequent shallow sampling at discrete stations where full-scale hydrographic measurements (including pH and total carbon dioxide) are performed. Shallow casts can be executed quickly and do not significantly reduce horizontal coverage.

Imagery and sea-truth data may be brought together in multidisciplinary (physical–chemical–biological) simulation models which link the appropriate variables and provide a mechanistic interpretation for both surface and subsurface observations. Because the horizontal features of the surface volume of interest are already present in the imagery, one-dimensional vertical models provide the important link between surface, mixed layer, thermocline and deeper waters. Figure 1 provides an artist's rendition of this approach.

Pigment and surface temperature

In upwelling areas, pigment, or chlorophyll-*a* concentration in the mixed layer computed from upwelled color, has been found to vary non-linearly with sea-surface temperature (Abbott and Zion, 1985). Pigment concentration appears to peak at an optimum temperature and is progressively less at lower and higher temperatures. For example, in waters off the coast of California, Abbott and Zion (1985) found that pigment concentration peaked at ~12°C. The same-shaped plot was observed in October 1985 by Zirino et al. (1988) for a 700 km transect of the Gulf of California, although the pigment maximum occurred at a temperature ~10° higher. The relationship can be explained as a series of states in a temporal upwelling–stratification sequence. Initially, cold, chlorophyll-poor, nutrient-rich water is brought to the surface by upwelling. Solar radiation then heats the water and promotes phytoplankton growth. Growth continues until stratification of the water column and/or advection away from the upwelling site reduce the flux of nutrients into the mixed layer, thereby causing the plankton concentration to decrease while

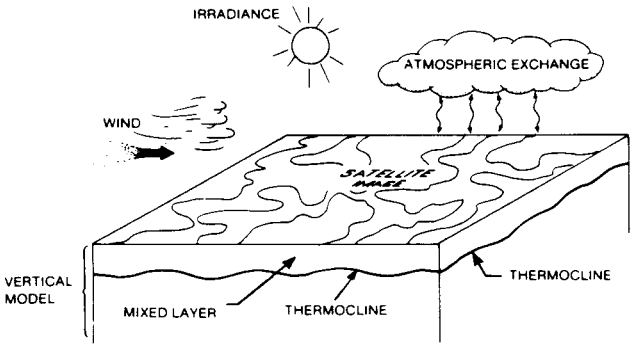

Fig. 1. Artist's conception of satellite imagery as a result of physical forcing.

temperature continues to increase to some steady-state value. This progression of events is shown diagrammatically in Fig. 2A and is presumed to hold for all waters in which stratification is controlled by temperature rather than salinity.

Figure 2A shows that pigment concentration increases exponentially from low to optimum temperatures and then decreases, again exponentially, at higher temperatures. Because of this exponential nature of the growth pattern, log pigment vs. temperature plots resemble the intersection of two straight lines with a sharp bend or "knee" at the intersection (Fig. 2B). In practice, however, the entire left-hand side of the plot is seldom, if ever, observed (new, cold water would need to surface extremely quickly) and the right-hand side of the plot predominates in most images. In a detailed study of northern California coastal waters, Abbott and Zion (1985) found that a relatively linear, inverse, log pigment–SST relationship existed in imagery collected at the site over several days, and they used the relationship to map out areas of positive or negative "anomalies" (higher or lower pigment than predicted by the relationship). Both kinds of anomaly were associated with large plumes streaming from the coast for 200–300 km.

pH, total carbon dioxide (TCO_2) and temperature

The pH of oceanic surface waters contains information which may be related to both temperature and chlorophyll-*a* concentration and thus to SST and pigment in imagery. In tropical waters, or in any waters where the density structure is determined by temperature, pH profiles tend to show the same

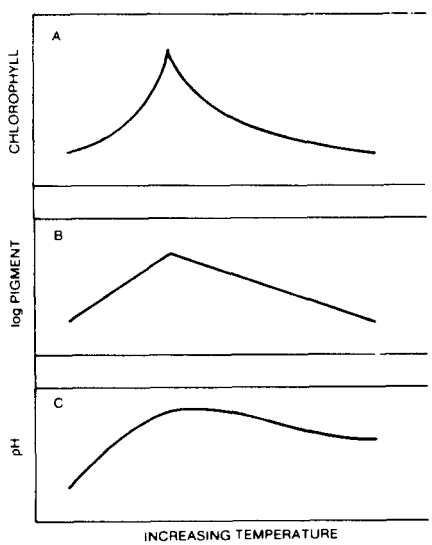

Fig. 2. Diagrammatic representation of chlorophyll concentration, log pigment, and pH at the ocean's surface as a function of increasing surface temperature.

features as temperature profiles (Zirino et al., 1986). Indeed, they are often linearly related, despite the fact that the pH profile contains *both* physical and biological information.

The reason for this is as follows: in the absence of biological processes, the pH of ocean water with a salinity of 34–36 ppt, measured at 1 atm. pressure and 25°C, would be $\sim 8.23 \pm 0.02$ (Zirino et al., 1986). This is the value attained when carbon dioxide gas, carbonic acid, bicarbonate and carbonate ions in the water reach equilibrium with atmospheric CO_2. In the euphotic zone, solar radiation warms the water and simultaneously drives photosynthesis which removes CO_2 and raises the pH, viz.,

$$HCO_3^- \rightarrow CO_2 + OH^- \quad (1)$$

On the other hand, in colder, aphotic (subsurface) water, respiration releases CO_2 and lowers the pH. Thus, warm surface waters tend to have a high pH, while deeper, colder waters have a pH < 8.2. When mixing masks in situ biological processes, temperature, pH, salinity, nutrients, etc., in the upper 100 m can be expected to be linearly related to each other, giving rise to similar (or mirror image) vertical profiles.

However, this covariation is misleading because pH and temperature are not directly related (the effect of temperature on pH in the ocean is small (Zirino et al., 1986)). For instance, there is no a priori reason for the surface water to both heat and increase pH via photosynthesis at a proportional rate. In fact, while mixing processes may be identical for both variables, in situ processes at the end points may be unrelated, with pH and temperature changing within their respective biological and physical constraints.

pH vs. temperature obtained from continuous measurements from underway ships may also produce characteristic plots, somewhat analogous to the pigment vs. temperature plots obtained from satellites. For example, consider the course of a ship from an area of newly upwelled water, through zones of increasing primary production but also progressive stratification, to a terminal area of high stratification and very low production. A plot of surface pH vs. surface temperature values collected on this transect could be represented by Fig. 2C. The lower, left-hand portion of the curve, that representing the "newest" upwelled water, is characterized by the lowest pH value, as well as the lowest temperature. The plot then shows a steep, positive slope as solar radiation heats the water and drives production. Finally, the slope decreases as productivity becomes limited by lack of nutrients, ultimately reaching a plateau where pH no longer increases, although temperature might still continue to increase.

Implicit in this conceptual model (Fig. 2C) are two assumptions: (i) pH is proportional to TCO_2 and changes in pH accurately reflect changes in TCO_2, and (ii) that TCO_2 is essentially conserved in the system, i.e. changes in TCO_2 from loss or gain across the air–sea boundary are small when compared with biologically produced effects. The first assumption appears well justified. Zirino et al. (1986) pointed out that a nearly linear relationship existed between

pH and TCO_2 if the specific alkalinity was held relatively constant. During the GEOSECS expeditions (Broecker et al., 1982) it was found that the specific alkalinity of Pacific surface waters was essentially constant at ~ 0.1197 and therefore pH and salinity could be used to predict TCO_2 to within $\pm 8 \mu M\,kg^{-1}$. While specific alkalinity in Atlantic surface waters was slightly more variable, TCO_2 could still be predicted from pH and salinity with high accuracy. Our own measurements in the North Atlantic and in the Gulf of California in 1985 substantiate this observation (Zirino et al., 1988).

The second assumption also appears to be justified. The velocity with which $CO_2(g)$ exchanges across the air–sea boundary is approximately ten times smaller than that of other gases in seawater. Broecker and Peng (1982) estimate that ~ 1 year is required for $CO_2(g)$ in the upper 50 m to reach atmospheric equilibrium. This period is much longer than the time required for a biological response to atmospheric forcing which occurs in periods of days or weeks. Since biological CO_2 changes are directly correlated with pH changes, it follows that the pH of surface water is often different from the "equilibrium pH" and much more indicative of in situ biological processes. It also follows that, because atmospheric exchange is slow, the pH of the surface water represents an integral of individual photosynthesis or respiration events occurring over days, weeks or, perhaps, months.

This is not to say that there is no $CO_2(g)$ exchange across the air–sea boundary, but that $CO_2(g)$ loss or gain to the atmosphere must be considered as part of a TCO_2 budget in which, generally, biological processes cause the greatest changes. Of course, where production is low, air–sea exchange becomes a significant if not predominant component of the CO_2 budget.

Multidisciplinary vertical models

The complex relationships between physical, biological and chemical variables observed in the field can be better understood by means of models which simulate the important time-dependent processes occurring in the oceans. Such models are driven by physical forces (solar radiation, winds, currents) which cause biological responses (photosynthesis, grazing) which, in turn, result in measurable chemical and biological changes (nutrients, chlorophyll, oxygen, CO_2). Unfortunately, while there are excellent working models in each discipline, there is, at present, no commonly accepted multidisciplinary vertical model.

The desire to understand better the interactions among common oceanographic variables at and near the ocean's surface led us to develop a relatively simple, multidisciplinary, vertical model which incorporates many of the features found in the single discipline models. The model is of the differential type, in the sense that the equations for heat, momentum, plankton, nutrients (nitrogen), oxygen and CO_2 are not integrated over the mixed layer. Rather, the surface layer is simulated by an arbitrary number of discrete layers with variable diffusivities between them. This type of model allows for high vertical

resolution, compatible with the resolution presently available with pump profiles of temperature, pH and chlorophyll (Fuhrmann and Zirino, 1988).

We have used the vertical model to understand better the shapes of pigment and pH vs. temperature plots for the Gulf of California. These plots were obtained from satellite imagery and horizontal transects sampled at sea during the Naval Ocean Systems Center's VARIFRONT III expedition to the Gulf of California during Nov.–Dec. 1981. This report presents and discusses our findings.

METHODS

Data collected at sea

pH and temperature measurements were made aboard the USNS deSteiguer on 10–11 December 1981. Water was obtained from a hull penetration in the scientific sea chest, ~ 3 m below the water's surface, and pumped into the ship's laboratory. pH, temperature and chlorophyll were measured continuously during the transect as described in Zirino and Lieberman (1985) and Lieberman et al. (1987). pH at 25°C was computed from the mV readings of the glass electrode and the temperature readings of the adjoining thermistor (Zirino and Lieberman, 1985).

Imagery

Color and thermal images were collected at the Scripps Satellite Oceanographic Facility (SSOF) of the Scripps Institution of Oceanography in La Jolla, California, on 16 and 17 November 1981, and archived and processed thereafter. Daytime thermal infrared data from channel 4 (11 μm) of the Advanced Very High Resolution Radiometer (AVHRR) on the NOAA-7 satellite were corrected for the effect of thin low clouds, using channel 2 (0.7–1.1 μm) near-infrared data (Gower, 1985), and then calibrated by an SSOF radiometric calibration procedure based on Lauritson et al. (1979). Multi-channel correction for absorption of sea-surface radiance by atmospheric water vapor was not employed because preserving the better signal-to-noise ratio of the single-channel data was more important than an accurate temperature estimate. Visible radiance data from the Coastal Zone Color Scanner (CZCS, on the Nimbus-7 satellite) were processed with an algorithm based on Gordon et al. (1983) to remove effects of Rayleigh and aerosol scattering and to derive pigment concentrations from corrected blue/green ratios.

Model

In the vertical model (Keir and Fiedler, 1988), heat and momentum are input by solar radiation and surface wind stress. Solar radiation is attenuated at

depth as a function of phytoplankton pigment concentration. Heat loss from the surface is a linear function of surface temperature. Nitrate flux is determined by upwelling and turbulent mixing. Phytoplankton growth is a function of light intensity, nitrate concentration and phytoplankton biomass. Light attenuation varies with phytoplankton biomass. Turbulent mixing is modeled as the product of the vertical gradient of a property and an eddy diffusion coefficient. Eddy diffusivity varies as a function of the gradient Richardson number (stratification/shear, Paconowski and Philander, 1981). Diffusion of oxygen and CO_2 through the sea surface is represented by the stagnant film model (Liss, 1975). Grazing is assumed to be a constant fraction of phytoplankton carbon per unit time. Phytoplankton grazed at a particular depth is redistributed at depth according to an exponential function, and remineralized, utilizing oxygen. Changes in carbon, oxygen, and nitrogen are linked by the Redfield ratio (Redfield et al., 1963).

A set of non-linear, partial differential equations represents conservation of mass, momentum and heat in the system. The Crank–Nicholson method is used to solve the set of equations in discrete form. The resulting set of algebraic equations takes on a tri-diagonal matrix form and the solution converges in one to three iterations at each time step. The user specifies the number of depth intervals and total depth of the water column to be modeled, as well as the time step, in days, for solution of the discrete equations. Initial concentrations of the variables upwelling velocity, surface wind speed, and surface light intensity are the inputs required at the start of a model run. The code is in QUICK BASIC and runs on an IBM personal computer or compatible instrument.

RESULTS AND DISCUSSION

Figure 3A,B shows the processed SST and pigment images of the Gulf obtained from satellite data collected on November 16 and 17. Temperature decreases and pigment concentration increases with degree of whiteness. The line leading from north to south approximates the track of the USNS DeSteiguer 24 days later. From the southern portion of the basin to just south of the two major islands, the IR image displays progressively colder temperatures, with the coldest water occurring southwest of Tiburon Island, where the topography shoals from a depth of ~ 1800 to 200 m. This zone of cold water persists throughout the year and coincides with the boundary between the shallow, northern region of ~ 200 m depth, and a deeper southern region (Fig. 4). Four major basins of progressively increasing depth (Guaymas, Carmen, Farallon and Pescadero) are sequentially located along the length of the southern Gulf.

Intense forcing by tides, winds, solar heating and exchanges with the Pacific Ocean promote a vigorous circulation, characterized in the south by large, deep, eddies and wind-driven coastal upwelling. Plumes of upwelled water

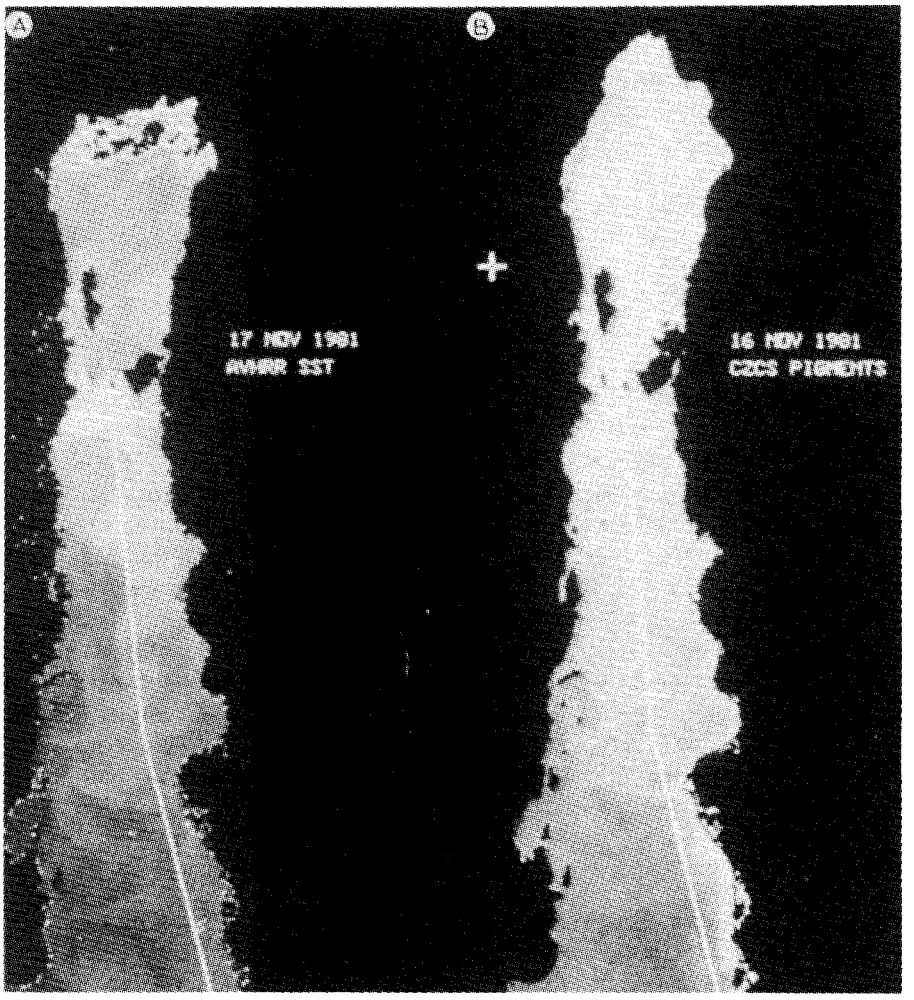

Fig. 3. Satellite imagery of sea-surface temperature (SST) and color imagery of the Gulf of California, Nov. 16–17, 1981.

stream from the coasts along the boundaries of the eddies. The direction of rotation of the eddies as well as the location of coastal upwelling (east, west) varies seasonally with the direction of the prevailing winds.

Figure 3A shows features typical of the surface thermal structure of late fall, winter and early spring (Badan-Dangon et al., 1985). This structure is notable for large, anticyclonic eddies extending across the Gulf in the Guaymas and Carmen Basins. Driven by a northwesterly wind, cold water upwells along the east coast and streams across the Gulf. On November 17, the coldest water ($\sim$ 19°C) was found south of Tuburon Island, streaming towards the west coast and forming the northern boundary of the Guaymas eddy. The eddy itself is

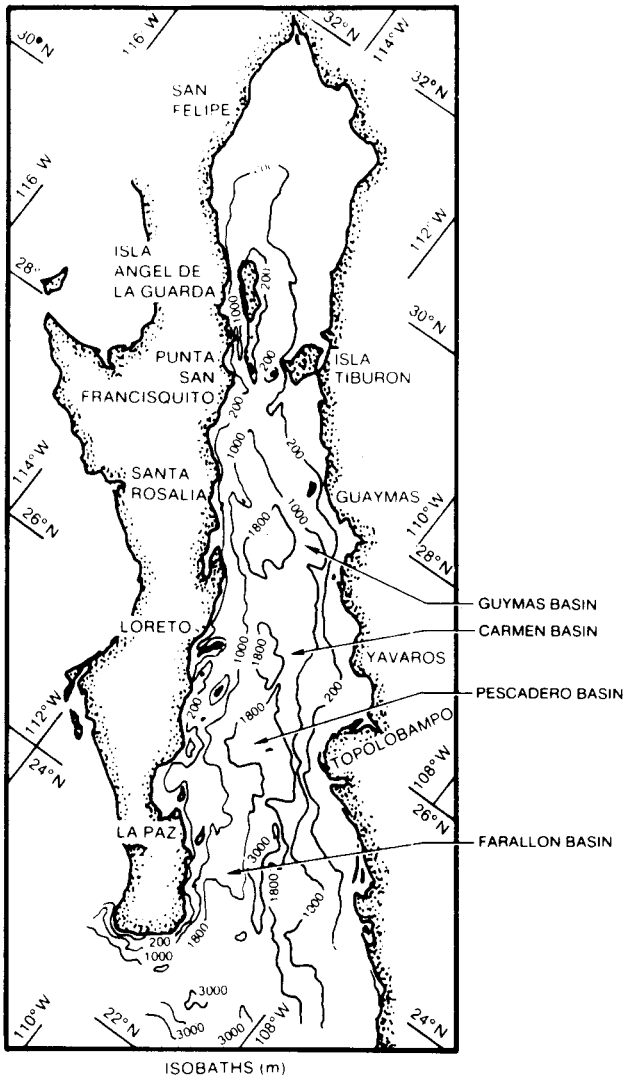

Fig. 4. Bathymetric chart of the Gulf of California.

split into two smaller eddies separated by a plume of 20.5°C water which emanates north of Guaymas and reaches west to Santa Rosalia. The southern boundary of the eddy is marked by a plume of ~22°C water which leaves the coast just south of Guaymas, reaches the center of the Gulf and then deflects southward to form a small cyclonic gyre. Several such small (~30–50 km) eddies mark the surface waters of the Carmen Basin, which have a mean temperature of ~23°C and which are separated from more southerly waters by a steep 1°C front radiating westward of Topolobampo.

The pigment image, Fig. 3B, shows spatial structure similar to that found in the IR image, although the pattern is less intense. A major difference is a 10 km wide, high-pigment zone which hugs the mainland coast. This zone, which has no temperature counterpart, is also found in 1985 Gulf imagery (Zirino et al., 1988). From south to north, pigment increases by about an order of magnitude, but this is somewhat obscured in the image which, as customary, is log-transformed.

Figure 5A displays log(pigment) along the north–south cruise track shown in Fig. 3. Pigment values range from $\sim 0.3\,\mu g\ l^{-1}$ in the south to $\sim 3\,\mu g\ l^{-1}$ in the north. Similarly, Fig. 5B displays SST along the same path. Figures 5C and D display the in-situ "surface" (actually 5 m) pH and temperature measured along the track on December 10–11, 3.5 weeks later. For comparison, the graphs have been drawn to the same horizontal scale. It is evident from the temperature plots that, despite some shifts in the relative positions of the eddies, the locations and temperatures of major features in the Gulf remained relatively unchanged during the 3.5 week period between the two data sets. While there is roughly a one degree absolute difference between the sets, they

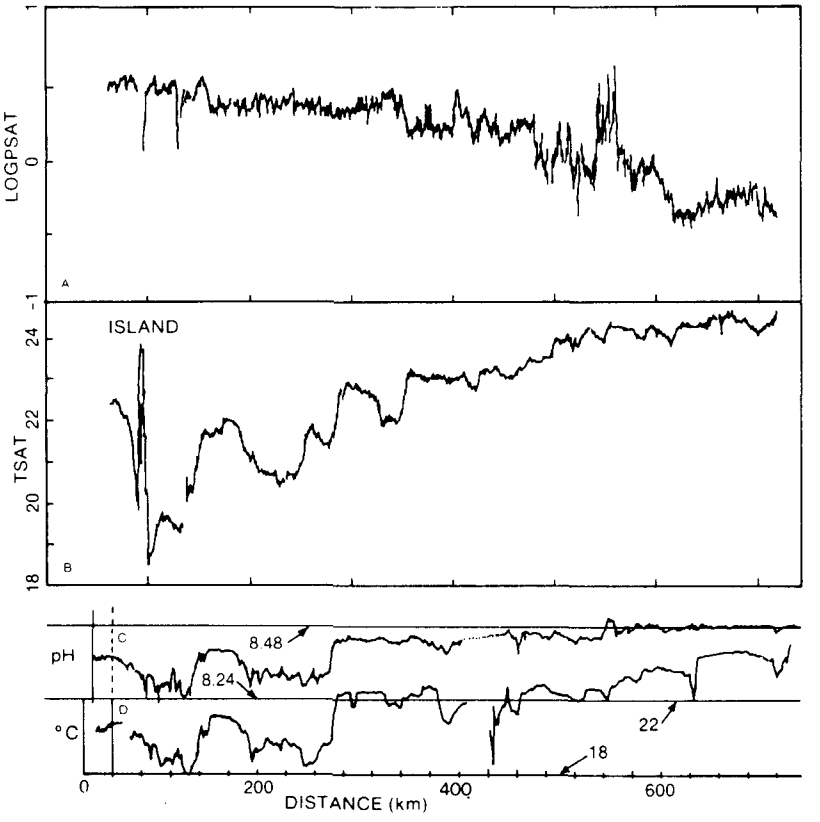

Fig. 5. Log pigment, SST, pH and in situ temperature of the Gulf of California, Nov.–Dec. 1981.

are in fact highly correlated, and a one degree difference between two such diverse measurements is not unexpected.

Figure 6(A,B) shows plots of log pigment vs. SST and pH vs. "surface" temperature measured at sea. In both plots there is a major change in slope occurring at ~22°C. This temperature marks the southern boundary of the eddy which occupies the Guaymas Basin and divides the Gulf into a high-pigment northern region and into a southern area of progressively lower pigment (and chlorophyll). pH is low in the high pigment region, increasing at a relatively rapid rate to ~8.47 and then leveling off at this value, in the southern, low-pigment zone. Zirino and Lieberman (1985) suggested that the

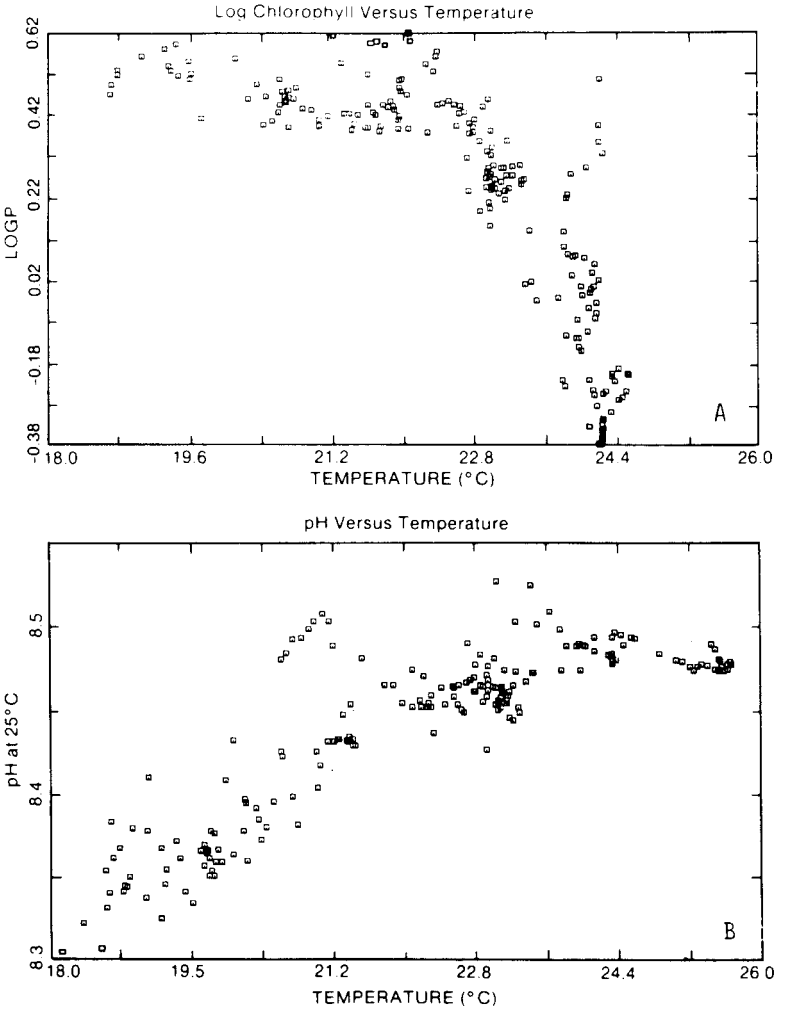

Fig. 6. (A) Log pigment vs. SST and (B) pH vs. in situ temperature. Gulf of California, Nov.–Dec. 1981.

increase in pH in the northerly region was the result of high primary production. Indeed, Baumgartner (1988) pointed out that, in the Gulf, primary production and chlorophyll concentration were linearly related.

The clear "break" in both plots at ~22°C suggests that log pigment and pH are related to temperature in the manner discussed earlier (Fig. 2) and that two different productivity regimes exist within the 800 km transect studied. It is not particularly clear, however, how the rate of change of chlorophyll standing stock with temperature relates quantitatively to the rate of change of pH or TCO_2 with temperature, since we did not measure any rates. Instead, the relationship between the two data sets was studied by means of the vertical model which relates all the time-dependent variables quantitatively.

Vertical model

Figure 7 shows time–depth plots of two runs of the model with 10 m layers

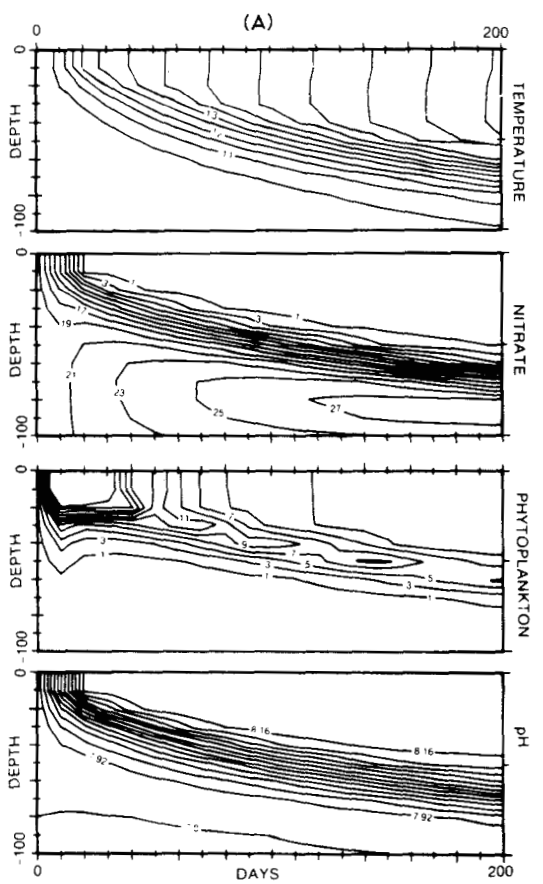

Fig. 7. Time–depth plots of model simulation. (A) Low mixing: upwelling = 0 m day^{-1}, winds = 2 m s^{-1}. (B) High mixing: upwelling = 0.5 m day^{-1}, winds = 5 m s^{-1}.

for 200 days: *low mixing*, with no upwelling and 2 m s^{-1} surface winds (Fig. 7A), and *high mixing*, 0.5 m day^{-1} upwelling and 5 m s^{-1} surface winds (Fig. 7B). Initial conditions are uniform profiles representing cold, deep water with low phytoplankton, low pH and high nitrate concentration. Low mixing, after 10 days, produces a mixed layer above a strong thermocline that continually deepens. A surface phytoplankton bloom peaks between 20 and 30 days and then declines, leaving a subsurface phytoplankton maximum, when nitrate is depleted in the mixed layer. High mixing produces a weaker thermocline which, because of upwelling, is more shallow than the first case. The surface phytoplankton bloom reaches a higher peak that declines more slowly. The vertical maximum phytoplankton biomass remains at the surface.

Figure 8(A, B) shows phytoplankton–temperature and pH–temperature plots from the two model runs. Since the model run was arbitrarily set to start at 10°C, differences in absolute temperature between the model run and the waters of the Gulf are not important. Although the two plots represent covariability in time, the same relationships will be observed in the spatial domain

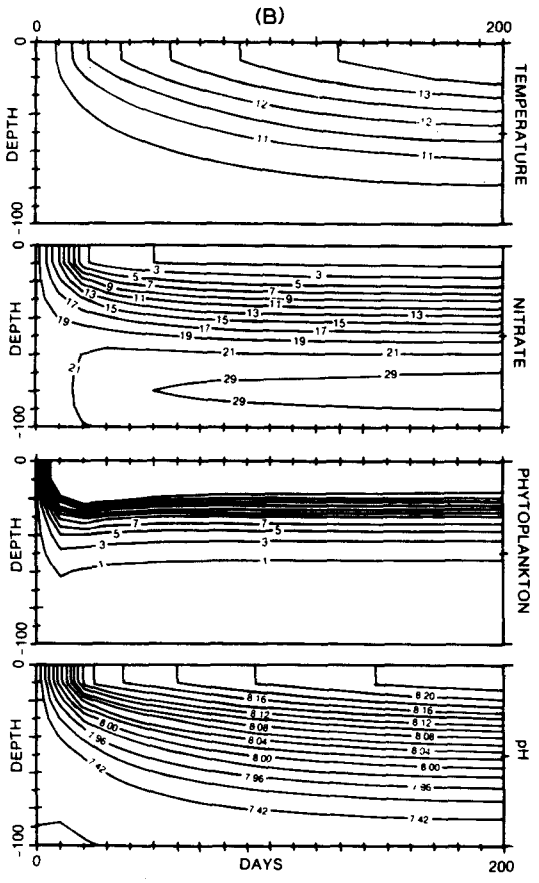

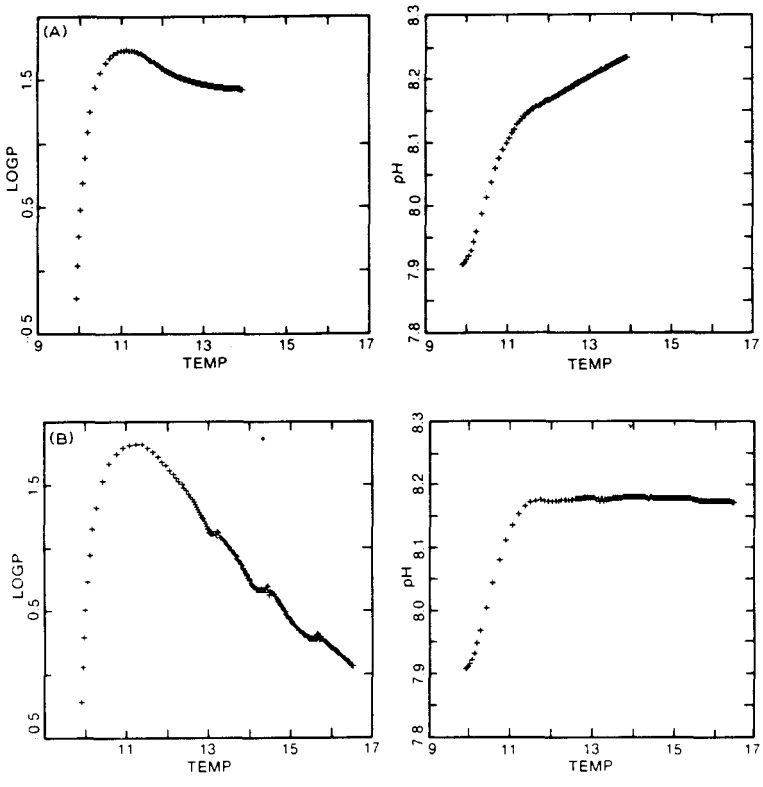

Fig. 8. Results of model simulation for surface waters. (A) Plots of log pigment and pH vs. surface temperature for high mixing condition. (B) Plots of log pigment and pH vs. surface temperature for low mixing condition.

if spatial variability is caused by asynchronous temporal cycling. Such asynchrony might be caused by upwelling at capes and banks or by local mixing events such as storms or breaking internal waves.

The most obvious feature of both plots for both runs is the break at 11–11.5°C. In this temperature range, nitrate drops to levels that significantly limit phytoplankton growth. Phytoplankton increases up to this temperature and then decreases above it. The negative slope of the phytoplankton–temperature plot above 11.5°C is much steeper in the low mixing run because mixed layer nitrate is lower and phytoplankton growth does not compensate for grazing and diffusion losses.

Initial pH in these runs corresponds to oversaturation of CO_2. Atmospheric equilibrium is not attained in either run. Phytoplankton growth accelerates the approach to equilibrium as the surface water warms. Thus, the different slopes of the pH–temperature plots above 11.5°C represent the different growth rates maintained after the initial surface bloom. In the high mixing run (Fig.

8A), pH continues to increase because nutrient input by upwelling and diffusion across the thermocline are sufficient to support continued net carbon fixation by photosynthesis. If the lapsed warming time of the water is substituted for the water temperature in Fig. 8, then the slope of the pH–time plot represents the net CO_2 fixed over the 200 days (minus the CO_2 lost by evasion). Of the two cases illustrated, the results produced by the low mixing case (Fig. 8B) more clearly resemble the plots obtained from the satellite imagery and underway data. The steep decrease in phytoplankton and leveling off of pH at higher temperatures suggest that stratification in the southern Gulf is instrumental in controlling production.

The satellite observation did not show the cold temperature (left) portion of the log pigment–temperature plot predicted by the model. This was as expected, since deep water, devoid of phytoplankton, does not instantaneously surface, as in the model. However, the imagery shows essentially constant phytoplankton over 4° of warming ($\sim$ 40–60 days). This suggests that the model does not fully simulate the observed conditions. Be that as it may, it is not our intention to model the Gulf of California accurately (a much more complete set of experimental data would be needed), but to point out that a comprehensive approach may serve to explore relationships among temperature, pH and chlorophyll on large spatial scales, with the ultimate purpose of assessing oceanic primary production remotely.

Finally, the examples presented here qualitatively illustrate how productivity rates, relative to the rate of heating of the surface water, are represented by the slopes of the phytoplankton–temperature and pH–temperature curves. To the extent that these surface variables change through biological responses to physical mixing, they can yield information about vertical movements within the near-surface water column. Thus satellite measurements of surface temperature and chlorophyll may also yield information about near-surface vertical structure.

ACKNOWLEDGEMENTS

We wish to thank Angela Rebello for giving us the opportunity to present this paper at the second Rio Conference on the Chemistry of Tropical Marine Systems. We are also grateful to Saul Alvarez-Borrego and Gilberto Gaxiola-Castro of the Centro de Ivestigaciones Cientificas y Escuela Superior de Ensenada (CICESE) for making VARIFRONT III possible and for many years of fruitful, happy, collaboration. Our thanks also go to Dr Eugene P. Cooper and NOSCs Internal Research Program for continuing support of work on oceanic pH. P.C. Fiedler was supported at NOSC by an Office of Naval Technology (ONT) postdoctoral fellowship. R.S. Keir was supported at NOSC by an ONT Summer Faculty fellowship. Finally, we wish to thank Susan Cola, Martha Stallard and Fabiola Rodriguez for their suggestions and support.

REFERENCES

Abbott, M.R. and P.M. Zion, 1985. Satellite observations of phytoplankton variability during an upwelling event. Cont. Shelf Res., 4: 661–680.

Badan-Dangon, A., C.J. Koblinsky and T. Baumgartner, 1985. Spring and summer in the Gulf of california: observations of surface thermal patterns. Oceanol. Acta, 8: 13–22.

Baumgartner, T., 1988. Ph.D. Thesis, Dept. of Oceanography, Oregon State University, Corvallis, OR 97331, U.S.A.

Broecker, W.S. and T.H. Peng, 1982. Tracers in the Sea. Eldigio Press, Palisades, New York.

Broecker, W.S., D.W. Spencer and H. Craig, 1982. GEOSECS Pacific Expedition, Vol. 3. U.S. Government Printing Office, Washington, DC.

Fuhrmann, R. and A. Zirino, 1988. High-resolution determination of the pH of seawater with a flow-through system. Deep-Sea Res., 35: 197–208.

Gordon, H.R., D.K. Clark, J.C. Mueller and W.R. Hovis, 1980. Phytoplankton pigments from the Nimbus-7 coastal zone color scanner: comparison with surface measurements. Science, 210: 63–66.

Gordon, H.R., D.K. Clark, J.W. Brown, R.H. Evans and W.W. Broenkow, 1983. Phytoplankton pigment concentrations in the Middle Atlantic Bight: comparison of ship determinations and CZCS estimates. Appl. Opt., 22: 20–36.

Gower, J.F.R., 1985. Reduction of the effect of clouds on satellite thermal imagery. Int. J. Remote Sensing, 6: 1419.

Keir, R.S. and P.C. Fiedler, 1988. A one-dimensional (vertical), interdisciplinary, oceanographic model for the personal computer. NOSC TP (in preparation).

Lauritson, L., G.G. Nelson and R.W. Porto, 1979. Data extraction and calibration of TIROS-N radiometers. National Oceanic and Atmospheric Administration, Technical Memorandum NESS 107, pp. 44–46.

Lieberman, S.H., D. Lapota, J.R. Losee and A. Zirino, 1987. Planktonic bioluminescence in the surface waters of the Gulf of California. Biol. Oceanogr., 4: 25–46.

Liss, P.S., 1975. In: J.P. Riley and G. Skirrow (Eds), Chemical Oceanography, Vol. 2. Academic Press Inc., London, p. 193.

Pacanowski, R.C. and S.G.H. Philander, 1981. Parameterization of vertical mixing in numerical models of tropical oceans. J. Phys. Oceanogr., 11: 1443.

Redfield, A.C., B.H. Ketchum and F.A. Richards, 1963. In N.M. Hill (Ed.), The Sea, Vol. 2. Wiley Interscience, New York, p. 26.

Zirino, A. (Ed.), 1985. Mapping Strategies in Chemical Oceanography. Advances in Chemistry No. 209. American Chemical Society, Washington, DC, 467 pp.

Zirino, A. and S.H. Lieberman, 1985. In: A. Zirino (Ed.), Mapping Strategies in Chemical Oceanography, Advances in Chemistry Series No. 209. American Chemical Society, Washington, DC, Chapt. 18, p. 393.

Zirino, A., R.A. Fuhrmann, D. Oksanen-Gooden, S.H. Lieberman, C. Clavell, P.F. Seligman, J.H. Mathewson, W.D. Jones, J. Kogelschatz and R.T. Barber, 1986. pH–temperature–nutrient relationships in the eastern tropical Pacific Ocean. Sci. Total Environ., 58: 117–137.

Zirino, A., R. Fuhrmann, K. Richter, J.R. Lara-Lara, G. Gaxiola-Castro and S. Alvarez-Borrego, 1988. An estimate of primary production from satellite imagery and hydrography in the Gulf of california (in preparation).